Multiresolution features for fingerpint image retrieval

Javier A. Montoya Zegarra, Neucimar J. Leite, and Ricardo da S. Torres
Institute of Computing
State University of Campinas
Av. Albert Einstein, 1216
Campinas, São Paulo, Brazil
{javier.montoya,neucimar,rtorres}@ic.unicamp.br

Abstract

This paper presents a real time system to guide the search and the retrieval in fingerprint image databases considering both retrieval accuracy and speed. For that purposes, we use multiresolution-based feature extraction and indexing methods considering the textural information inherent to fingerprint images. The extracted feature vectors are used to compute the distance between the fingerprint query image to all the fingerprints in the database and the N most similar images are then retrieved. The focus of this work is to study the utility of multiresolution transforms on the domain of fingerprint recognition.

1. Introduction

Biometrics, which refers to the automatic recognition of individuals by their physical and/or behavioral characteristics, has emerged as a motivating and instigating research field [13]. In fact, several biometric applications have been adopted in civilian, commercial and forensic areas. Traditionally, the physical characteristics used for human recognition include: fingerprints [10], iris [24], retina [9], and face [25], while the behavioral ones include: signature [19], voice [5], and gait [2].

Among all these biometric characteristics, fingerprints are considered one of the most reliable characteristic for human recognition due to their individuality and persistence [20]. The fingerprint's individuality means that it is unique across individuals and across fingers of the same individual, even in identical twins [12]. On the other hand, the fingerprint's persistence means that the basic fingerprint characteristics do not change with time.

The popularity of fingerprint-based recognition have led to large-scale databases. While the large size of these collections compromise the retrieval speed, the noise and the distortion that can be found in fingerprint images may reduce the overall retrieval accuracy. Therefore, both retrieval accuracy and speed play an important role in the fingerprint recognition process.

Roughly speaking, there are two kinds of approaches that can be employed to reduce the retrieval speed, namely exclusive and continuous classification. The former uses some high-level characteristics to partitionate the fingerprint database into mutual exclusive bins. Once the fingerprint query image is classified, it will be searched only in its corresponding bin. In the latter, the fingerprint images are represented by feature vectors. Similarities among fingerprint images are established by the distance in the feature space of their corresponding feature vectors. This approach is closely related to a fingerprint database indexing problem.

The objective of both approaches is to characterize the fingerprint images by some global information for indexing purposes, instead of offering some kind of discriminatory information for recognition. Typically, the global information is obtained by studying the patterns in the central region of the fingerprints formed by their ridge structure. In this context, we propose an original continuous approach to guide the search and the retrieval in fingerprint image databases. We study particularly the textural patterns presented in the central region of fingerprints in order to generate feature vectors used for fingerprint indexing and retrieval. In our approach, the texture features are extracted by multi-scale transforms: Steerable Pyramid (SP [6]) and different types of the Wavelet Transform, which include: Gabor Wavelet Transform (GWT [14, 18]) and Tree-Structured Wavelet Transform (TSWT) using Orthogonal (Haar, Daub 4-Tap, Daub 8-Tap and Daub 16-Tap [3, 17]) and Bi-orthogonal (Spline [22]) Filterbanks.

In the case of the Steerable Pyramid different orientation filters and decomposition levels are used to generate a translation and rotation-invariant fingerprint representation. In the GWT, different scales and orientations are used to capture the relevant texture information, whereas in the TSWT the image texture content is captured on the low frequency subband, while the high frequency subbands are used to capture the image variations in different directions.

The remainder of this paper is organized as follows. Next section presents the contributions of our work, while section 3 reviews some related approaches. Section 4 presents the architecture of our system. The module used for detecting the center point region of the fingerprints is presented in section 5. The various features extracting algorithms are described in section 7. The premilinary results of our experiments, are discussed in section 8. Finally, our conclusions are described in section 9.

2. Objectives and Contributions

Although search spaces can be reduced in exclusive classification approaches, there are some shortcomings that should be considered: (1) some fingerprints present properties of more than one class and therefore they cannot be assigned into just one bin, (2) the natural distribution of fingerprints is not uniform and therefore even performing binning in the original database, the number of one-to-many comparisons can still be high, and (3) some of the fingerprint characteristics used for binning are not easy to detect due to the presence of noise and distortions. Therefore, there are still some open questions that should be answered, such as: (1) is it possible to reduce the searching space considerably without classifying fingerprints? (2) which fingerprint information should be considered for that purposes? (3) how can be the query processing time improved? and (4) how can fingerprint images stored and indexed efficiently?

In our work, we plan to address these opening challenges. For that purposes, we propose a method to characterize fingerprints by using feature vectors to summarize their principal textural and directional properties. The fingerprint candidates are then retrieved from the database by comparing the distance of their feature vectors. The smaller the distance is, the more similar the images are. Theoretically, our approach will present the following advantages over exclusive classification: (1) since fingerprints are represented by feature vectors, then the ambiguity of classification is resolved, because they are not represented by a single class, (2) depending on the accuracy expected for the system, some parameters referred to search radius and number of nearest neighbors can be configured and adjusted, and (3) continuous classification can be treated as a fingerprint image retrieval problem and therefore we want to prove the suitability of Content-based Image Retrieval (CBIR) techniques for fingerprint indexing and retrieval.

3. Related Work

To the best of our knowledge, there are mainly two works that address the problem of fingerprint identification as a fingerprint database indexing problem.

Germain et al. [7] proposed a continuous system to index fingerprint databases using flash hashing. Their system is composed by two associative memory structures, namely, multimap and map. During the fingerprint feature extraction process, some information related to the feature vectors is generated in order to create indices that could be the same for different fingerprints. Each of these indices is then added to the multimap memory structure. During the retrieval process, each of the generated indices of the query image is used to retrieve the image candidates, that are presented by the same indices. The map memory structure is then used to store the references of the image candidates together with some parameters that characterize the geometric transformation between two pairs of feature vectors as well as a score value used for sorting the list of image candidates. The feature vectors are composed by a set of triplets (x, y, θ), where the three parameters represent the location and orientation of each of the minutiaes. In order to create a more robust method, they also considered the number of ridges between minutiaes. Thus, a set of triangles that resemble one another can be constructed. The number of matching triangles serves as the basis for determining whether two pair of fingerprints are the same or not. They showed also that by using this approach the average query time decreased mainly due to the reduction of I/O operations.

Another example is the work proposed by Tan [21]. It presents a comparison between an exclusive and a continuous classification method. For the exclusive classification method, they used Genetic Programming to generate some compositing operators that are applied to the features extracted from the orientation field of the image. For classification purposes, a Bayesian classifier was used. The fitness parameter value was adjusted considering the classification result. The continuous classification method used, followed the work proposed by Germain et al. [7]. The main difference is that their system has two steps, instead of just one. As a result of the indexing process, a list of candidates is retrieved according to the similarity between feature values. For verification purposes only the top N candidates are used. The identification score is calculated as the number of corresponding triangles between the query image and the candidates. The triangles are formed by the location of the minutiaes. They also concluded that the search space and the false acceptance rate (FAR) were reduced when com-

paring the continuous classification method with the exclusive one.

Although the search spaces are reduced in both approaches ([7, 21]), they are mainly based on some singularities presented in fingerprint images. Besides, the accurate detection of these singularities depend highly on the quality of the fingerprint images and their computation often involves some computational resources that will affect directly the fingerprint recognition time. On the other hand, they both use flash hashing for indexing purposes and we believe that by using metric access methods the query processing time will be improved. Thus, as seen in Table 1, we will consider more specifically the textural and directional information presented in fingerprints for feature extraction purposes, since they both retain the discriminating power of fingerprints and Metric Access Methods for their indexing.

4. System Overview

The architecture of our proposed framework, presented in Figure 1, can be divided into two main subsystems, namely, the enrollment- and the query-subsystem. The enrollment-subsystem acquires the information that will be stored in the database for later use. On the other side, the query subsystem is responsible for retrieving similar fingerprints from the database according to the user's fingerprint query image. Our system operates as follows:

1. Enrollment-subsystem: several fingerprint images are first captured (arrow labeled 1 in Figure 1) and a Region of Interest (ROI) within the fingerprint is marked (module 1, arrow 2) by a center point area detection module. A region of 64×64 pixels is used for marking the ROI. The feature extraction algorithms contained in the descriptor library (module B, arrow 3) are used by the feature extraction module to generate the features (arrow 4) that are indexed by a metric access method for further use.
2. Query-subsystem: a fingerprint query image is received as input from the user (arrow 1). Once, the fingerprint ROI is detected (module A, arrow 2) the feature extraction algorithms contained in the descriptor library are used to extract the feature vectors from the query image (module B with arrows 3 and 4, respectively). The query image feature vector is used to rank the database images according to their similarity to the query image (module C). For that purposes, a distance computation algorithm is selected from the descriptor library (arrow 5) and the metric access method is used to speed up the retrieval (arrow 6). Finally, the most similar database images are ranked (arrow 7) and returned to the user (arrow 8).

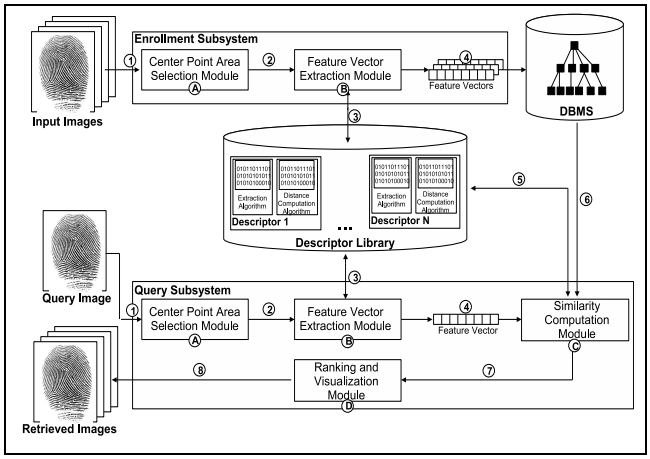

Figure 1. Architecture of our proposed system.

5. Center Point Area Detection

In order to detect the fingerprint center point area, we first locate the core point, that correspond to the uppermost point contained in the inner-most ridge line. We have chosen the core point as the basis of the center area detection, because: (1) it mostly appears in the central part of the fingerprint and, (2) is more frequently than deltas [23]. The steps used for core detection are [11]:

1. Estimation and smoothing of the directional fields of the fingerprint input image.
2. Computation of the Poincaré index, in each (8×8) block. This index is defined as follows:

$$\text{Poincare(i,j)} = \frac{1}{2\pi} \sum_{k=0}^{N-1} \Delta(k) \tag{1}$$

$$\Delta(k) = \begin{cases} \delta(k) & \text{if } |\delta(k)| < \frac{\pi}{2} \\ \pi + \delta(k) & \text{if} \delta(k) \leq -\frac{\pi}{2} \\ \pi - \delta(k) & \text{otherwise} \end{cases} \tag{2}$$

$$\delta(k) = \theta(X(k^{'}), Y(k^{'})) - \theta(X(k), Y(k)) \tag{3}$$

where $k^{'} = (k+1) \bmod (N)$ and $\theta(i,j)$ is the directional field of the fingerprint image. $X(k)$ and $Y(k)$ are the coordinates of the blocks that are in the closed curve with N blocks. If the Poincaré index has a value of 1/2, then the current block is the core block. The

center of this block is then the core point. If more than two cores are detected, go back to step 1 using a larger smoothing parameter for the directional fields.

Once the center point is obtained, a center point area can be easily defined. An image of size 64×64 pixels around the core point is then cropped.

6. Multiresolution Methods

In this section, we present the multiresolution methods used for capturing the textural information presented in the fingerprint center point area.

6.1. Steerable Pyramid

The Steerable pyramid is a linear multi-orientation and multi-scale image decomposition method, by which an image is subdivided into a collection of subbands localized at different scales and orientations [6]. This decomposition transform is based on convolution and decimating operations and has the advantage that the subbands are translation- and rotation-invariant. Using a high- and low-pass filter (H_0, L_0) the input image is initially decomposed into high- and low-pass subbands. The low-pass subband is further decomposed into a total of k-oriented band-pass portions $B_0, \ldots, B_k$ and into a lowpass subband L_1. The recursive decomposition is done by subsampling by a factor of 2 along the rows and columns the lower low-pass subband. The decomposition process of the first level of the Steerable Pyramid is shown in Figure 2.

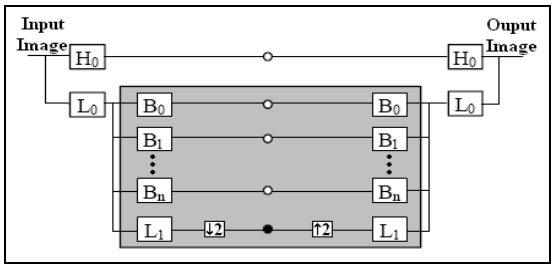

Figure 2. First Level of Steerable Pyramid Decomposition.

6.2. Tree-Structured Wavelet Transform

The Wavelet Transform is computed by applying a pair of filters (a lowpass filter H and a highpass one G) to a signal and then by downsampling the filtered signals by a factor of two. A discrete two dimensional Wavelet transform can be defined as:

$$L_j = \Big[H_x * [H_y * L_{j-1}]_{\downarrow 2,1}\Big]_{\downarrow 1,2} \quad (4)$$

$$D_{j1} = \Big[H_x * [G_y * L_{j-1}]_{\downarrow 2,1}\Big]_{\downarrow 1,2} \quad (5)$$

$$D_{j2} = \Big[G_x * [H_y * L_{j-1}]_{\downarrow 2,1}\Big]_{\downarrow 1,2} \quad (6)$$

$$D_{j3} = \Big[G_x * [G_y * L_{j-1}]_{\downarrow 2,1}\Big]_{\downarrow 1,2} \quad (7)$$

where the operator * refers to the convolution operator, $\downarrow_{2,1}$ ($\downarrow_{1,2}$) represent the image downsampling along the rows and columns and $L_0 = I$ is the original image. L_j represent the low resolution image at scale j obtained by lowpass filtering. D_{ji} / $i \in \{1, 2, 3\}$ are the detail images obtained by highpass filtering and they contain directional detail information at scale j. Thus, a multi-scale representation of depth d of the image I can be build considering the subimages at several scales: L_d, D_{ji}, where $i = \{1, 2, 3\}$ and $j = \{1, 2, \ldots, d\}$ [4].

In the TSWT, it is possible to decompose recursively the output of each of the subbands ($L_d, D_{j1}, D_{j2}, D_{j3}$) [1]. For the sake of pattern retrieval, a fixed decomposition structure is convenient, since if facilitates distance computations and hence database browsing. Considering that the subband D_{j3} leads often to unstable features, recursively decomposition is done in the other subbands.

6.3. Gabor Wavelet Transform

A general 2-D Gabor function $\psi(x, y)$ is defined as:

$$\psi(x, y) = \left(\frac{1}{2\pi\sigma_x\sigma_y}\right) exp\left[-\frac{1}{2}\left(\frac{x^2}{\sigma_x^2} + \frac{y^2}{\sigma_y^2}\right) + 2\pi jWx\right] \quad (8)$$

where the spatial coordinates (x, y) denote the centroid localization of the elliptical Gaussian window. The parameters σ_x and σ_y are the space constants of the Gaussian envelop along the x- and y-axes, respectively. The Fourier transform $G(u, v)$ of the Gabor function $\psi(x, y)$ can be written as:

$$G(u, v) = exp\left[\frac{-1}{2}\left(\frac{(u - W)^2}{\sigma_u^2} + \frac{v^2}{\sigma_v^2}\right)\right] \quad (9)$$

where W represents the frequency of the sinusoidal plane along the horizontal axis and the frequency components in x- and y-direction are denoted by the pair (u, v), while $\sigma_u = 1/2\pi\sigma_x$ and $\sigma_v = 1/2\pi\sigma_y$. Considering the non-orthogonal basis set formed by the Gabor functions, a localized frequency description can be obtained by expanding a signal with this basis.
Self-similar class functions, known as Gabor Wavelets,

can be generated by dilations and rotations of the mother wavelet $\psi(x, y)$, i.e.:

$$\psi_{m,n}(x, y) = a^m \psi_{x',y'}, \qquad a > 1 \tag{10}$$

considering $m = 1, \ldots S$ and $n = 1, \ldots K$. S and K denote the total number of dilations and orientations, respectively, and:

$$\begin{bmatrix} x' \\ y' \end{bmatrix} = a^{-m} \begin{bmatrix} cos\theta_n & sin\theta_n \\ -sin\theta_n & cos\theta_n \end{bmatrix} \begin{bmatrix} x \\ y \end{bmatrix} \tag{11}$$

where $\theta = n\pi/K$ and θ is the rotation angle. To ensure that the energy is independent of m, a scale factor a^{-m} is introduced. Considering the redundant information presented in the filtered images due to the non-orthogonality of the Gabor Wavelets, Manjunath et al. [18] designed a strategy to reduce the redundancy of the Gabor Wavelets Filterbank, where the half-peak magnitude of the filter responses touch each other in the frequency spectrum:

$$a = \left(\frac{U_h}{U_l}\right)^{\frac{1}{S-1}} \qquad \sigma_u = \frac{(a-1)U_h}{(a+1)\sqrt{2ln2}} \tag{12}$$

$$\sigma_v = tan\left(\frac{\pi}{2K}\right)\left[U_h - 2ln2\left(\frac{\sigma_u^2}{U_h}\right)\right]\left[2ln2 - \frac{(2ln2)^2\sigma_u^2}{U_h^2}\right]^{-\frac{1}{2}} \tag{13}$$

where $W = U_h$. The parameters U_h and U_l are used, respectively, to denote the upper and lower center frequencies of interest.

7. Feature Extraction

To generate the feature vectors some statistical measures are used to compute the feature vectors. More precisely, the mean μ_{mn} and the standard deviation σ_{mn} of the energy distribution of the multiresolution transform coefficients are used to capture the fingerprint textural information and thus to form the feature vector f:

$$\mu_{mn} = \frac{1}{MN} \iint |W_{mn}(x, y)|\, dx\, dy \tag{14}$$

$$\sigma_{mn} = \sqrt{\iint (W_{mn}(x, y) - \mu_{mn})^2\, dx\, dy} \tag{15}$$

Considering $k = 16$ orientation subbands and $l = 6$ decomposition levels, the feature vector for the case of the Steerable Pyramid is generated as follows:

$$\vec{f_{SP}} = [\mu_{11}, \sigma_{11}, \mu_{21}, \sigma_{21}, \ldots, \mu_{k1}, \sigma_{k1}, \mu_{1l}, \sigma_{1l}, \mu_{2l}, \sigma_{2l}, \ldots, \mu_{kl}, \sigma_{kl}] \tag{16}$$

For the Tree-Structured Wavelet Transform the values of $|W_{mn}(x, y)|$ correspond to the energy distribution in one of the three subbands: LL, LH, and HL. Thus, the subindices *m* and *n* are integers that stand for the decomposition level and the current subband ($m = 1, 2, \ldots, L$ and $n = 1, 2, 3$), respectively. The feature vector $\vec{f}$ is formed as follows:

$$\vec{f_{TSWT}} = [\mu_{11}, \sigma_{11}, \mu_{12}, \sigma_{12}, \mu_{13}, \sigma_{13}; \ldots; \mu_{L1}, \sigma_{L1}, \mu_{L2}, \sigma_{L2}, \mu_{L3}, \sigma_{L3}] \tag{17}$$

In the case of the Gabor Wavelet Transform, the values of $|W_{mn}(x, y)|$ denote the energy distribution of the transform coefficients after convolving an image I with the Gabor Wavelet $\psi_{m,n}$. Considering a total number of S=6 scales and K=16 orientations, the resulting feature vector is computed as follows:

$$\vec{f}_{GW} = [\mu_{11}, \sigma_{11}; \mu_{12}, \sigma_{12}; \ldots \mu_{6\,16}, \sigma_{6\,16}] \tag{18}$$

8. Preliminary Results and Conclusions

Preliminary results of our work include a comparative study of different textural image descriptors used for fingerprint indexing and retrieval. The main objective of our experiments was to study the possibility of reducing the fingerprint retrieval speed by reducing image search spaces using the fingerprints textural information. For that purposes, we have explored different combinations of multiresolution and texture-based feature extraction algorithms with similarity measures.

The multiresolution-based feature extraction algorithms also include: Steerable Pyramid and six different types of the Wavelet Transform: Gabor Wavelets and Tree-Structured Wavelet Transforms using Haar, Daubechies (Daub 4-Tap, Daub 8-Tap and Daub16-Tap), as well as, the Spline Wavelets. The translation- and rotation-invariant representation of the Steerable Pyramid is an important issue for the fingerprint domain, whereas, the different spatial/frequency subimages integrated naturally by the Wavelet Tranform has demonstrated good performance for texture analysis [15].

For computing the distance among the generated feature vectors, we have studied different similarity measures which include: Bray-Curtis, Canberra, Euclidian, Manhattan, Square Chord and Square Chi-Squared distance.

Our study was conducted on each of the four databases presented in the FVC 2000 Database [16]. The retrieval effectiveness of our approach was measured in terms of the precision and recall curves [8]. Considering the query image q and the number of correct, missed and false candidates (n_c, n_m and n_f, respectively), the precision p_q in the first R retrieved images is defined as follows:

$$p_q = \frac{n_c}{n_c + n_f} = \frac{n_c}{R} \tag{19}$$

while the recall r_q of the such similar candidates S of the query image q is defined as:

$$r_q = \frac{n_c}{n_c + n_m} = \frac{n_c}{S} \tag{20}$$

Our system was tested independently in each of the four databases and each of the fingerprint images was considered as a query image, thus, a total number of 880 fingerprint queries were performed. For each query, the precision and recall curves were computed for the 8-Nearest Neighbors. Figures 3, 4, 5, and 6 show the best retrieval accuracy combination between multiresolution feature extraction methods and similarity measures for each of the four databases.

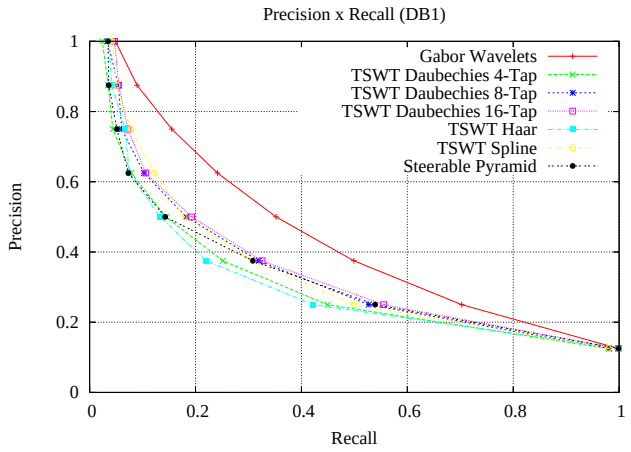

Figure 3. Average Precision vs. Recall curves of the best image descriptors for the DB1.

9. Conclusions

In this work we presented a novel approach for fingerprint indexing and retrieval by using different multiresolution techniques and similarity measures. The retrieval accuracy was measured in terms of precision and recall curves. Preliminary results show that the best retrieval accuracy was achieved by the Gabor Wavelet Transform combined with the Square Chord similarity measure.

10. Acknowledgments

This work was partially financed by CNPq, CAPES, FAEPEX, FAPESP, CNPq WebMaps and Agroflow projects, and supported by Microsoft eScience grant. Javier Montoya is grateful to CNPq (134990/2005-6).

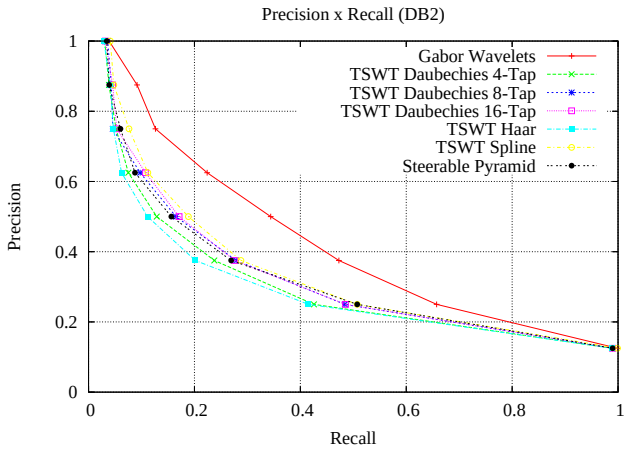

Figure 4. Average Precision vs. Recall curves of the best image descriptors for the DB21.

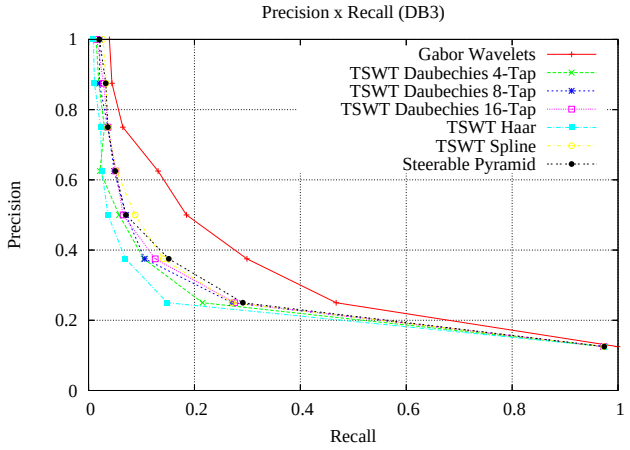

Figure 5. Average Precision vs. Recall curves of the best image descriptors for the DB3.

References

[1] T. Chang and C.-C. J. Kuo. Texture analysis and classification with tree-structured wavelet transform. *IEEE Transactions on Image Processing*, 2(4):429–441, October 1993.

[2] B. Chiraz, C. R. G., and D. L. S. Gait recognition using image self-similarity. *EURASIP Journal on Applied Signal Processing*, 2004:572–585, 2004.

[3] I. Daubechies. The wavelet transform, time-frequency localization and signal analysis. *IEEE Transactions on Information Theory*, 36(5):961–1005, September 1990.

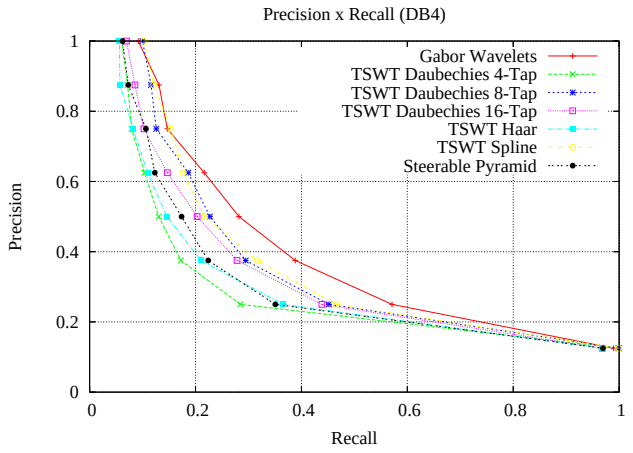

Figure 6. Average Precision vs. Recall curves of the best image descriptors for the DB4.

[4] G. V. de Wouwer, P. Scheunders, and D. V. Dyck. Statistical texture characterization from discrete wavelet representations. *IEEE Transactions on Image Processing*, 8(4):592–598, April 1999.

[5] A. Eriksson and P. Wretling. How flexible is the human voice? - a case study of mimicry. *Proceedings of EUROSPEECH*, 2:1043–1046, 1997.

[6] W. T. Freeman and E. H. Adelson. The design and use of steerable filters. *IEEE Transactions on Pattern Analysis and Machine Intelligence*, 13(9):891–906, 1991.

[7] R. S. Germain, A. Califano, and S. Colville. Fingerprint matching using transformation parameter clustering. *IEEE Computational Science and Engineering*, 4(4):42–49, December 1997.

[8] W. I. Grosky, R. Jain, and R. Mehrotra, editors. *Handbook of Multimedia Information Management*. Prentice-Hall, 1997.

[9] Hill-99. *Retina Identification, Biometrics: Personal Identification in Networked Society*. Kluwer Academic, 1999.

[10] A. K. Jain, L. Hong, S. Pankanti, and R. Bolle. An identity-authentication system using fingerprints. *Proceedings of the IEEE*, 85(9):1365–1388, September 1997.

[11] A. K. Jain, S. Prabhakar, and L. Hong. A multichannel approach to fingerprint classification. *IEEE Transactions on Pattern Analysis and Machine Intelligence*, 21(4):348–359, 1999.

[12] A. K. Jain, S. Prabhakar, and S. Pankanti. On the similarity of identical twin fingerprints. *Pattern Recognition*, 35(11):2653–2663, November 2002.

[13] A. K. Jain, A. Ross, and S. Prabhakar. An introduction to biometric recognition. *IEEE Transactions on Circuits and Systems for Video Technology*, 14(1):4–20, January 2004.

[14] T. S. Lee. Image representation using 2d gabor wavelets. *IEEE Transactions on Pattern Analysis and Machine Intelligence*, 18(10):959–971, 1996.

[15] K.-C. Liang and C.-C. Kuo. Waveguide: a joint wavelet-based image representation and description system. *IEEE Transactions on Image Processin*, 8(11):619–1629, November 1999.

[16] D. Maio, D. Maltoni, R. Cappelli, J. L. Wayman, and A. K. Jain. Fvc 2000: Fingerprint verification competition. *IEEE Transactions on Pattern Analysis and Machine Intelligence*, 24(3):402–412, 2002.

[17] S. G. Mallat. A theory for multiresolution signal decomposition: the wavelet representation. *IEEE Transactions on Pattern Analysis and Machine Intelligence*, 11(7):674–693, July 1989.

[18] B. S. Manjunath and W.-Y. Ma. Texture features for browsing and retrieval of image data. *IEEE Transactions on Pattern Analysis and Machine Intelligence*, 18(8):837–842, August 1996.

[19] V. S. Nalwa. Automatic on-line signature verification. *Proceedings of the IEEE*, 85(2):215–239, February 1997.

[20] S. Pankanti, S. Prabhakar, and A. K. Jain. On the individuality of fingerprints. *IEEE Transactions on Pattern Analysis and Machine Intelligence*, 24(8):1010–1025, 2002.

[21] X. Tan, B. Bhanu, and Y. Lin. Fingerprint identification: classification vs. indexing. *Proceedings of the IEEE Conference on Advanced Video and Signal Based Surveillance*, pages 151–156, July 2003.

[22] M. Unser, A. Aldroubi, and M. Eden. A family of polynomial spline wavelet transforms. *Signal Processing*, 30(2):141–162, 1993.

[23] F. Wang, X. Zou, Y. Luo, and J. Hu. A hierarchy approach for singular point detection in fingerprint images. *Lecture Notes in Computer Science*, 3072:359–365, January 2004.

[24] R. P. Wildes. Iris recognition: An emerging biometric technology. *Proceedings of the IEEE*, 85(9):1348–1363, September 1997.

[25] W. Zhao, R. Chellappa, P. J. Phillips, and A. Rosenfeld. Face recognition: A literature survey. *ACM Computing Surveys*, 35(4):399–458, December 2003.